

Surrogate models for the blade element momentum aerodynamic model using non-intrusive Polynomial Chaos Expansions

Rad Haghi¹ and Curran Crawford¹

¹Institute for Integrated Energy Systems, University of Victoria, British Columbia, Canada

Correspondence: Rad Haghi (rhaghi@uvic.ca)

Abstract. In typical industrial practice based on IEC standards, wind turbine simulations are computed in the time domain for each mean wind speed bin using a few number of unsteady wind seeds. Software such as FAST, BLADED or HAWC2 can be used to capture the unsteadiness and uncertainties of the wind in the simulations. The statistics of these aeroelastic simulations output are extracted and used to calculate fatigue and extreme loads on the wind turbine components. The minimum require-
5 ment of having six seeds does not guarantee an accurate estimation of the overall statistics. One solution might be running more seeds; however, this will increase the computation cost. Moreover, to move beyond Blade Element Momentum (BEM)-based tools toward vortex/potential flow formulations, a reduction in the computational cost associated with the unsteady flow and uncertainty handling is required. This study illustrates the unsteady wind aerodynamic statistics' stationary character based on the standard turbulence models. This character is shown based on the output of National Renewable Energy Lab (NREL) 5MW
10 Blade Element Momentum (BEM) simulations. Afterwards, we propose a non-intrusive Polynomial Chaos Expansion (PCE) to build a surrogate model of the loads' statistics, NREL 5MW rotor thrust and torque, at each time step, to estimate the extreme statistics more accurately and efficiently.

1 Introduction

The process of calculating loads on wind turbine components is one of the core parts of wind turbine aerodynamic and structural
15 design and optimization. In the last few decades, international organizations have developed different aeroelastic codes such as Fatigue, Aerodynamics, Structures, and Turbulence (FAST) (Jonkman et al., 2005), BLADED (Bossanyi, 2003) and HAWC2 (Larsen and Hansen, 2007) to accurately calculate load time series based on the standardized or site-specific environmental conditions. Engineers and researchers use wind turbine aeroelastic simulation output statistics to calculate extreme and fatigue
20 loads on wind turbine structure and estimate the unsteady power. To take into account the randomness in the unsteady wind, according to IEC standards (IEC 61400-1), the simulation process must use a semi Monte Carlo (MC) method. Therefore, a full simulation set should include a limited number of seeds for generating multiple wind speed time series of 600s.

In normal practice, for each mean wind speed, at least six different seeded unsteady wind time series are required as the minimum to take into account the uncertainties. This limited number of unsteady simulations does not yield an entirely accurate estimation of the statistics. Gradient-based optimization algorithms may not deal with these inaccuracies well. One option to
25 solve this problem is running more seeds, which will increase the computational cost. The increase in computational cost will

play a more critical role in our decision making if we want to move towards vortex (van Garrel, 2003) and potential flow codes for load calculations, as they require more computation resources inherently. An alternative approach to direct simulation is to use a surrogate model that can provide us with an accurate statistical estimation set based on a limited number of simulations.

The origin of the *surrogate model* lies in Uncertainty Quantification (UQ) analysis (Sudret, 2007). There are many uncertainty quantification implementations in wind energy. More specifically, surrogate models show much potential in wind farm load estimation, wind turbine optimization or reliability analysis. Many researchers have investigated these potentials. For example, Dimitrov et al. (2018); Schröder et al. (2018); van den Bos et al. (2018); Dimitrov (2019) used surrogate models to estimate the loads on a wind turbine based on the stochastic variables gross parameters such as turbulence intensity, mean wind or wind direction. Ashuri et al. (2016); Murcia et al. (2018); Schröder et al. (2020a) used surrogate models for uncertainty propagation through the wind turbine models. More recently, the surrogate models have been used for the wind turbines reliability assessments (Slot et al., 2020; Schröder et al., 2020b). Also, Wang et al. (2020) and Barlas et al. (2021) showed the application of surrogate model in wind turbine optimization. However, very few have looked at building a surrogate model of the aerodynamic model of wind turbine based on the random phases as the input. Fluck and Crawford showed an initial attempt to build a surrogate model based on intrusive Polynomial Chaos Expansion (PCE) on simple lifting line and BEM models (Fluck and Crawford, 2016a, 2018). As they were quickly faced with *curse of dimensionality*, they showed it is possible to reduce the number of random variables in Veers' unsteady wind model significantly. Afterwards, they used this reduced dimension wind model to propagate stochasticity through a simple lifting line (Fluck and Crawford, 2016b) or BEM (Fluck and Crawford, 2018) model. However, with intrusive PCE it is necessary to change the model implementation fundamentally to incorporate the random variables (Sudret, 2007). This might work for a simple model, but when we want to utilize commercially available aeroelastic codes, this will be challenging or even impossible.

This paper's goal is to build a non-intrusive PCE surrogate model of a deterministic aerodynamic model driven by stochastic unsteady wind. This study's implemented aerodynamic model takes wind time series as input and calculates thrust and torque on a NREL 5MW turbine rotor using BEM. The motivation is building a surrogate model based on a small number of simulations to be able to estimate the statistics of the aerodynamic model output at each time step of the time series quickly. As the surrogate models are inherently cheap to run, we take this surrogate model through a Monte Carlo Simulation (MCS) large number of times. The input of these MCS are the samples drawn from the uniform random variables. The unsteady wind generator uses the same random variable distribution to make sure the generated time series will match a Gaussian process (Veers, 1988). This process is presented in Figure 1 schematically. By this method, we can reduce the computational cost and time for the aerodynamic simulation, without compromising the validity of the results. One can interpret this model as a tool to map the input distribution (in this case, an uniform distribution of random seeds-phases) to the output distribution (in this case, distribution of thrust and torque on the rotor).

Fitting a surrogate model at each time step of 600s of the aerodynamic output times series, using the random phases (Figure 1), is computationally expensive and redundant to current practice. Therefore, we start by showing that the aerodynamic simulation results based on Veer's reduced model (Fluck and Crawford, 2017) statistically converges. We also show that the unsteady wind aerodynamic process's statistical properties are constant in time (stationary process). Therefore, by keeping

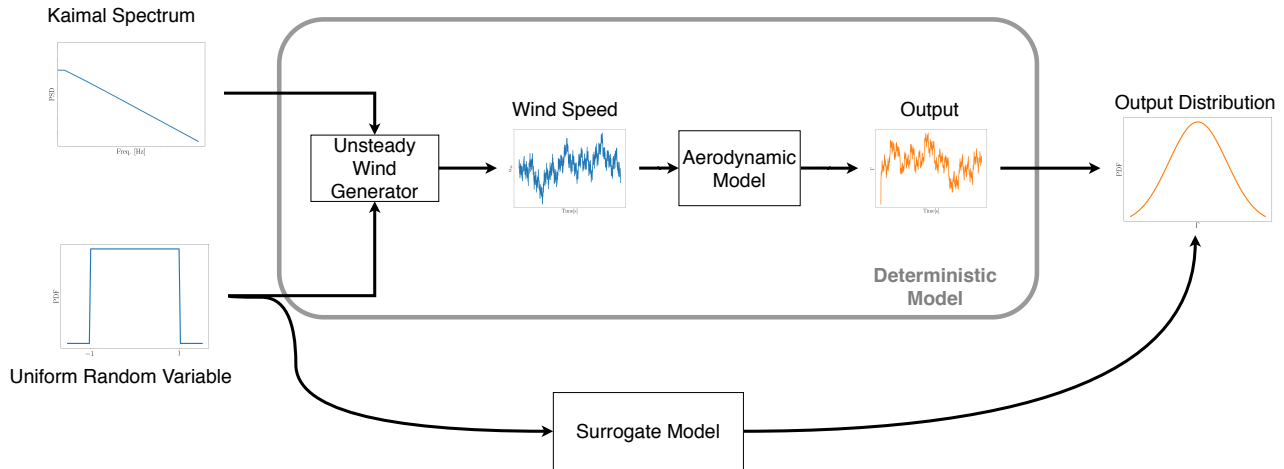


Figure 1. The common deterministic process of aerodynamic modeling vs the suggested surrogate model method schematic flow chart.

the computational effort the same, it is possible to run more simulations while shortening the length of the simulations. Furthermore, more simulations with the same computational effort give us the chance to fit higher degree PCEs, which provides a more accurate estimation of the statistics. We build four different PCEs surrogate models, with four different polynomial degrees (degrees two to five) to pick the best in terms of accuracy and computational cost trade-off. These surrogate models have been used for MCS for a large number of runs (cheaply). The results of the MC runs of the surrogate models are compared with 48000 unsteady wind aerodynamic simulation results. In this case, the simulation results are the thrust and torque forces induced on the NREL 5MW in an unsteady wind. We compare the results by looking at the thrust and torque distribution from both the deterministic and surrogate models. Finally, we show how the extreme loads extracted from the MCS can converge to the extreme loads from the results from 48000 unsteady wind aerodynamic simulation results.

This paper is organized as follows. Section 2, describes the unsteady wind generation, aerodynamic, statistical elements and PCE method used in the study. This section finishes by describing the approach to tackle the challenge. Section 3 provides the BEM simulation results, convergence of the sectional statistics the PCE fit on the sectional statistics and the emulations output. Finally, this section discusses the accuracy and efficiency of the surrogate models. This paper concludes in Section 4 which includes this study conclusion and the recommended future work.

75 2 Methodology

This section provides an overview of the unsteady wind generation basics and statistical elements used in this study. Afterwards, we explain the simulation and PCE method that we use in this study.

2.1 Reduced Veers unsteady wind model

One famous unsteady wind model in the wind turbine community is the Veers model (Veers, 1988). The history of the model goes back to the late 80s' and has a long record in wind turbine load calculation practice. Very briefly, Veers unsteady wind model is inherently an inverse Fourier transformation. The 1-D unsteady wind time series at location P is generated via:

$$u_{\infty}(t_n) = \sum_m \sqrt{S_m} e^{i(\omega_m t_n + 2\pi \xi_m)} \quad (1)$$

For this inverse Fourier transformation in Eq (1), the frequencies ω_m and are taken from the Kaimal spectrum (Figure 1). The random phases are based on the independent random variable ξ_m drawn from a uniform distribution over $[0, 1]$. Finally, the amplitude S_m is specified based on the power spectrum at the frequencies ω_m (Bossanyi et al., 2011).

In load calculation practice, Veers' model for the unsteady wind is the method to generate turbulent boxes, commonly implemented in TurbSim (Jonkman, 2009). The method is briefly explained in Fluck and Crawford (2017) and extensively in Veers (1988). To make the unsteady wind in TurbSim, this method uses a large number of random variables on the order of thousands is required Jonkman (2009). This large number of random variables pushes the surrogate model problem into the *curse of dimensionality* very quickly. Therefore, building a PCE surrogate model is almost impossible. To tackle this issue, Fluck and Crawford (2016b) showed that using only ten uniformly distributed independent random variables with ten frequencies logarithmically sampled from the Kaimal spectrum (Veers, 1988) is enough for building unsteady wind time series. This *Reduced Veers' model* generated unsteady wind that can capture the same level of randomness and probability distribution as the full model. This study used this reduced Veers model to generate unsteady wind time series. This method does not lead to a model that fully replaces high fidelity Turbsim outputs but rather a surrogate model necessity to study trade-offs of various accuracy and assumption aspects.

2.2 Aerodynamic model

The aerodynamic model for this study is a simplified BEM model (Bossanyi et al., 2011) with frozen wake based on the work of Lupton (2019) is employed. This non-linear BEM model is used to run simulations on a NREL 5MW Jonkman et al. (2009) rotor to calculate thrust and torque on the rotor. For the simulations, the rotor speed was kept constant based on the mean wind speed of the simulations. Also, the pitch angle was set according to the data provided in Jonkman et al. (2009). There is no controller involved in the simulations. The unsteady wind defined in the previous section is set at 100m hub height and remains the same on the rotor. The Python package for BEM is `bemused` (Lupton, 2019). The NREL 5MW model characteristics and properties are extracted from Jonkman et al. (2009). The model employed in this study for the simulations and surrogate model is essentially equivalent to the NREL 5MW model in any wind turbine aerodynamic code (e.g. FAST, BLADED and HAWC), but nicely formulated in Python. The model and analysis code used in this work has been previously verified against the NREL 5MW full model using BLADED by Lupton (Lupton, 2015).

2.3 Statistical convergence

For this study, we want to investigate if the cross-sectional statistics (statistics at each time step) of a combination of a large number of aerodynamic simulation outputs are similar or not. In other words, we want to investigate if the statistical properties of the output at each time step converge as a function of the number of simulations (stationary process) for the non-linear stochastically autocorrelated system. Figure 2 presents a generic example of distributions (histogram fits) at each time step for a set of realizations of one random process. (The figure shows a schematic plot; therefore, histograms and fitted distributions *do not* represent the plotted trajectories.) To show that the sectional statistics of a large number of simulations are convergent, we need a metric to quantify the difference between the distributions at each time step. There are different metrics for this purpose (Basu et al., 2011); for this study, we use *Hellinger distance* (Hellinger, 1909) as a metric due to its ease of application and interpretation. The Hellinger distance is a metric to quantify how two probability distributions are similar to each other. The distance is zero if they are the same and is one when the two distributions are disjoint. The Hellinger distance for two *discrete* probability distributions of P and Q , which have an equal number of bins, can be formulated as:

$$H(P, Q) = \frac{1}{\sqrt{2}} \sqrt{\sum_{i=1}^k (\sqrt{p_i} - \sqrt{q_i})^2} \quad (2)$$

In Eq.(2), p_i and q_i are the probabilities for P and Q at every bin. In our case, to make the comparison fair, not only the number of bins are the same, but also the bin width is the same for both P and Q . This assures us that there is no artificial distance reduction in the results.

In this study, we use Hellinger Distance to show the cross-sectional statistics changes for a large number of simulations is minimal. Therefore, we can shorten the simulations without losing the accuracy of the sectional statistics.

2.4 Polynomial Chaos Expansion

Uncertainty propagation of mathematical models has been the subject of many studies in the last thirty years. One method to propagate uncertainty is using models of models, called surrogate models. A surrogate model is a cheap-to-run approximation of the actual model (Kim and Boukouvala, 2019). Among the surrogate models, Polynomial Chaos Expansion (PCE) has gained attention especially after the work of Ghanem and Spanos (2003) and Xiu and Karniadakis (2003). PCE is a method that uses a variable with its uncertainty (random variable ξ) and projects the model onto a basis of polynomials. This way, the uncertainty can be propagated through the model with a limited number of simulations (Tyson et al., 2015). In other words, PCE is a technique to estimate the response of a mathematical or numerical model based on a series of orthogonal polynomials, which are functions of a random variable ξ . The solution is expanded and described in stochastic space spanned by ξ and the associated polynomial basis.

The main reasons to use PCE instead of other surrogate model methods are; a) with minimum computational effort, one can extract statistical moments directly from PCEs; b) PCEs are easy to integrate into deterministic linear and non-linear

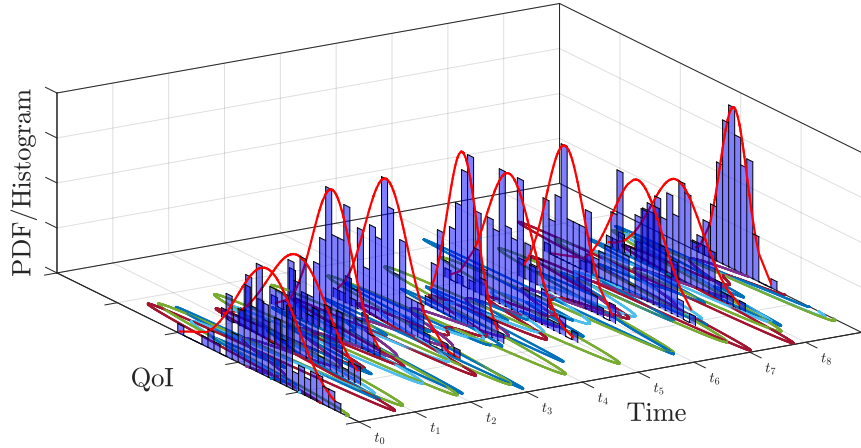


Figure 2. A schematic drawing presenting possible distributions at each time step based on a set of time trajectories for a Quantity of Interest (QoI)

mathematical models; c) one can build PCE surrogate model by treating the model as a black box (Kaintura et al., 2018; Sudret, 2015).

140 In order to make it easier to explain, let's assume $Y(t_n) = M(t_n, \boldsymbol{\xi})$ where t_n is time step n , and $\boldsymbol{\xi}$ is the random variable vector, $M(t_n, \boldsymbol{\xi})$ is our deterministic time marching mathematical model and $Y(t_n)$ is the output of the model in time step n . Therefore, the stochastic output of the model $Y(t_n, \boldsymbol{\xi})$ can be expanded as:

$$Y(t_n, \boldsymbol{\xi}) = \sum_{i=1}^{\infty} y_i(t_n) \Psi_i(\boldsymbol{\xi}) \quad (3)$$

145 where $y_i(t_n)$ are PCE coefficients at *each time step* and $\Psi_i(\boldsymbol{\xi})$ is a member of an orthogonal polynomial class. These polynomials are orthogonal with respect to the probability space of random variable $\boldsymbol{\xi}$. The selection of the polynomial type is a function of the probability distribution on the random variable $\boldsymbol{\xi}$. For example, if a random variable $\boldsymbol{\xi}$ has a normal distribution, then a Hermite polynomial is selected (Xiu and Karniadakis, 2002).

The polynomials do not necessarily need to be selected from the specific polynomials family as long as they are orthogonal polynomials. For instance, Fluck and Crawford (2018) showed exponential components worked best for their purposes. As the randomness in this study comes in the form of a uniform distribution for wind frequency component phases ϕ_j , the surrogate model is based on the Legendre polynomials (Xiu and Karniadakis, 2003). In practice, the PCE summation in Eq (3) is truncated

150

at a reasonably high order p . The task of fitting the expansion in Eq (3) is finding the coefficients $y_i(t)$. There are two main approaches to solve this problem:

- the *intrusive* approach where the model is projected on the orthogonal polynomials using Galerkin projection (Ghanem et al., 2017). This approach requires building a detailed stochastic model from the deterministic model governing equations. The intrusive approach was used by Fluck and Crawford (2016b, 2018) to build a surrogate model on a lifting line and BEM models.
- the *non-intrusive* approach allows calculating the PCE coefficients from a series of deterministic model evaluations. This approach considers the model as a black box and does not require any model modification (Sudret, 2007; Eldred et al., 2008). There are two sub-categories to calculate the coefficients, namely *simulation methods* and *quadrature methods* (Sudret, 2007).

The presented work uses the *non-intrusive* approach to calculate the PCE coefficients. In the non-intrusive approach categories we used a *simulation method* to calculate the PCE coefficients. In mathematical form, the output of the aerodynamic model $M_{aero}(t_n, \xi)$ at time step n is thrust $Trt(t_n)$ and torque $Trq(t_n)$. Therefore, one can re-write Eq. (3) as:

$$Trt(t_n, \xi) \approx \sum_{i=1}^m T_i(t_n) \Psi_i(\xi) \quad (4)$$

$$Trq(t_n, \xi) \approx \sum_{i=1}^m \tau_i(t_n) \Psi_i(\xi) \quad (5)$$

where the goal is to calculate the polynomial coefficients $T_i(t_n)$ and $\tau_i(t_n)$ at each time step. This surrogate model's input is the random variable ξ vector used in the reduced Veers model to generate the unsteady wind. The surrogate model's output is the thrust and torque at a specific time step for which the surrogate model is built. The main difference between Eq. (3) and (4)(5) is the approximation sign, as it is not feasible to take into account an infinite number of polynomials. This work's surrogate model is built employing the Python toolbox Chaospy (Feinberg and Langtangen, 2015). Chaospy is a numerical tool for uncertainty quantification using different methods, including PCE. For this study, we used the *point collocation* method to calculate the coefficient due to the ease of implementation in the Chaospy toolbox. This method has been explained well in the literature (see Xiu et al. (2002), Ghanem and Spanos (2003), Sudret (2007)).

2.5 Random variable sampling

The randomness in the generated unsteady wind comes from the ten random variables, ϕ_j , in ξ vector describing the frequency components' phases $2\pi\xi_m$ in the reduced Veers model in Eq. (1) (Fluck and Crawford, 2017). Based on the Veers method (Veers, 1988) and in TurbSim (Jonkman, 2009), the employed sampling method is a pseudo-Random Number Generator (pRNG) which is the basis of MCS. However, the problem with this way of sampling for MCS is the lack of control on the random variables' domain as it may fill some voids in the domain and may leave some of it empty (Niederreiter, 1992).

Therefore, the random domain may not be filled evenly for the same reason. For this study, a low discrepancy Quasi Monte Carlo (QMC) sampling method, namely the Sobol sequence (Sobol', 1967) is used to draw samples from the random variables in this work to calculate the PCE coefficients via point collocation method. The main reasons to select Sobol sequence over other sampling methods are the samples' consistency and computational efficiency (Kucherenko et al., 2015). A custom random
 185 wind generator based on the reduced Veers model used these samples to generate unsteady wind.

2.6 Approach

In this piece of work, whenever we talk about simulations, we mean aerodynamic simulations in time using the aerodynamic model introduced above. The input of the aerodynamic simulations is what we call wind time series or unsteady wind and is auto-correlated by construct. This wind time series is generated based on the reduced Veers model explained above.

190 This study starts with running an extensive set of simulations based on the reduced Veers model at $12m/s$ mean wind speed, aerodynamic simulation model and Sobol sampling, explained previously. This wind speed is the rated power wind speed for NREL 5MW. Afterwards, as we have a large number of simulations output in our database, we can show that the thrust and torque statistics with time are not changing significantly. Therefore the statistical process properties at each time step (e.g. mean, standard deviation, etc.) would be significantly similar to other time steps. Knowing the process statistics stays the same
 195 in times, we conclude that only building a single surrogate model, i.e., a single time-step or a few ones, would suffice for our purpose. The accuracy of the PCEs depends on the polynomial degree. However, an increase in the polynomial degree pushes the problem further toward the *curse of dimensionality*. The number of required coefficients to build the surrogate model and the required number of simulations are presented in Table 1. Eq (6) presents the formula to calculate the number of PCE coefficients. In Eq. (6), M is the required number of coefficients, N is the number of random variables, and P is the
 200 polynomial order.

$$M + 1 = \frac{(N + P)!}{P!N!} \quad (6)$$

The table shows we need a large number of simulations to build an accurate PCE. According to Hosder et al. recommendation, twice the number of simulations can provide acceptable accuracy for the point collocation method (Hosder et al.). That recommendation is the basis for the number of simulations in this study.

205 We want to limit the computational cost for a single average wind speed to 6 times 600s simulations (in total 3600s) to be competitive with the standard practice in wind turbine aerodynamic simulation. Combining a large number of simulations and 3600s cumulative simulations length leads to a large number of short simulations instead of a few long ones. We kept the simulation's cumulative length at 3600 seconds to make this trade-off fair. This means that as the simulations' length decreases, the number of simulations increases. Sobol sampling is the base of the unsteady wind generation and input to the aerodynamic
 210 simulation setup. For every set of the required number of simulations in Table 1, the random phases are drawn independently from the rest of the sets. For example, for the second row of Table 1, when we need 132 simulations, 132 unique samples of ξ are drawn from the random domain. These ξ have not been used for other simulation sets. By having a large number of data

Table 1. The number of coefficients and required data points to calculate the coefficients for 10 random variables and using the point collocation method. This number of coefficients should be calculated for every time step. The last column demonstrates the simulation length for the fitted PCEs as explained in Section 3.

Polynomial Degree	Number of Coefficients + 1	No of Required simulations	Sims. Length to fit PCEs [s]
1	11	22	163.6
2	66	132	27.3
3	268	536	6.7
4	1001	2002	1.8
5	3003	6006	0.6

points at each time step, we built a few surrogate models in time and compared the results with the simulations' reference case. For the sake of accuracy, in this study, we do not build any surrogate model based on 1st-degree polynomials.

215 Another approach to calculate the coefficients is Gaussian Quadrature (GQ). This method has been extensively explained in the literature e.g. Le Maître and Knio (2010). The reason we did not use GQ is the number of evaluation points required for this method. Our tests show that for a GQ method with 10 random variables and polynomial order 4 we would need 9765625 evaluation points. On the other hand, the Smolyak sparse approach for GQ (Le Maître and Knio, 2010; Smolyak, 1963), will reduce the number of evaluation points drastically to 10626. However, this is still five times more evaluation points than the
220 point collocation method used in this study. Future work may revisit the use of sparse and collocation methods for computing polynomial coefficients.

For a stationary input (Reduced Veers model), the sample statistics of output converges at the rate of $1/\sqrt{n}$, where n is the number of data points (in this case, 48000 data points at one time instance). Consequently, it is possible to *estimate* the statistical parameters of the output distribution by different methods; such as using the maximum likelihood estimator Rao
225 (2008). A question that then arises is why we go through the complication of building a surrogate model. The research goal we present here is building a surrogate model of an aerodynamic model, whether the aerodynamic model is simple or complex. We chose an aerodynamic model that is easy to simulate while complex enough to capture the inherent non-linear behaviour. Hence, the initial aerodynamic example model's simplicity does not compromise the validity of the method we introduce here to later more complex simulations with e.g. FAST or BLADED.

230 3 Results

This section presents the results of our numerical experiments. We start by looking at the Hellinger distance of a large number of aerodynamic simulation output, thrust and torque, and show the distance does not change significantly. Therefore, the sectional statistics are almost the same. Afterwards, based on that conclusion, we built a limited number of surrogate models for polynomial orders of 2 to 5 and show the statistics match the reference case. Finally, we show how extracted extreme thrust
235 and torque are comparable with the reference case.

3.1 Hellinger distance

As mentioned before, in Section 2, we started by running a broad set of reference simulations. For this case, we ran 48000 simulations for a $12m/s$ wind speed and turbulence intensity of 0.16. The wind generator code took 48000 samples from a 10 dimensional uniform distribution domain based on the quasi-random sampling method. Each sample is a 10 by 1 vector of ξ_j , and we have 48000 of them. 48000 wind speed time histories were generated, and simulations on the aerodynamic models run with a time step of $0.1s$ for $630s$ (in total 6300 time steps per simulation), with $30s$ transient period. We discarded the transient period for all the processes in this study.

This simulation setup builds a database for the investigation and shows that the process distributions at each time step changes are insignificant. Initially, we started calculating the histogram at each time step with identical binning for all of them. Afterwards, using the Hellinger distance formulation, each histogram's distance to the other histograms (5999 other histograms) was calculated and stored in a matrix. Each row of this matrix shows the histogram difference at one time-step compared to the other ones. Therefore, this is a symmetric matrix with zeros on the diagonal. What is important is the maximum of all of the data in the matrix; in Figure 3a and 3b, we show the max of the Hellinger distance at each time step for the aerodynamic model simulation outputs. The Hellinger distance is a normalized metric, and the distances are shown in the percentage. The plot shows a comparison of all the 18 million possible combinations to calculate the Hellinger distance for each model output. For the simulation outputs (thrust and torque), the distributions' difference does not exceed 0.0085%. This shows a strong coherence in the statistics at each time step. Therefore, we can conclude that building a surrogate model on a limited number of time steps, or even one time step, is enough, and it is not necessary to create a surrogate model on every time step as predicted by the aerodynamic model form.

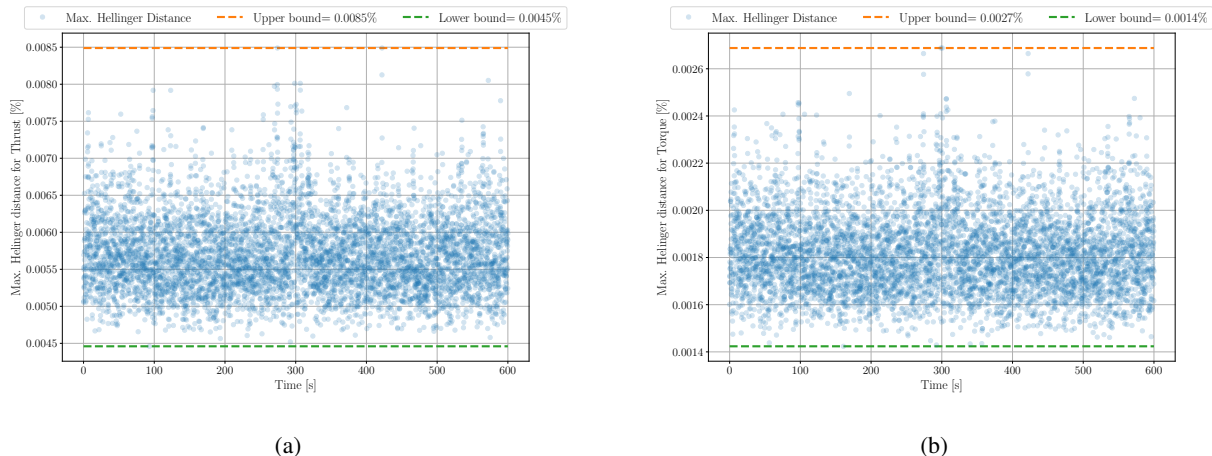


Figure 3. Maximum Hellinger distance for thrust and torque at each time step. The upper and lower bounds for the *extreme* of the Hellinger distance are indicated.

255 3.2 Surrogate model and emulation

We use the same simulation setup as explained above for the reference case to run the specified number of simulations in Table 1. These simulations are input for building the surrogate models. The number of samples drawn from the 10 dimensional uniform random space is equal to the number of simulations in Table 1. The employed sampling method is Sobol, as tests show it provides a better convergence for the PCE.

260 Referring to Figure 3, and the discussion in Section 3.1, the changes in statistical properties at each time step are minimal. Therefore, one surrogate model that can accurately emulate the sectional statistics of the aerodynamic simulations' output would suffice. Knowing this means building surrogate models is more feasible from a computational cost perspective.

As explained in Section 2, we fit surrogate models at every time step of a large set of short simulations instead of a few long ones for increasing polynomials order P . The number of simulations is based on the polynomial order as shown in Table
265 1. The length of the simulations that the surrogate model is built on every time step is the last column in Table 1 to keep the cumulative length of the simulations at 3600s. Although it was unnecessary, for polynomial degrees 3 to 5, we build surrogate models at every time step of the whole 10s worth of simulations to have an acceptable sample size for direct comparison. The Chaospy (Feinberg and Langtangen, 2015) toolbox was used to perform the task of building these surrogate models.

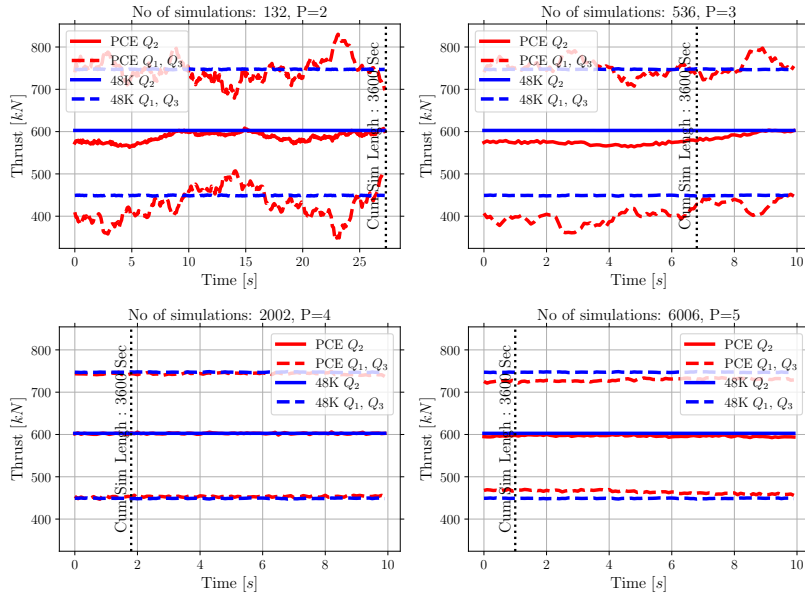
Figure 4 compares the descriptive statistics (first quartile Q_1 , second quartile Q_2 and third quartile Q_3) for both thrust and
270 torque from the reference case with 48K simulation outputs and 48K MCS of the surrogate model build at each time step. The results in Figure 4 show the PCE fits for four polynomial degrees; P on each plot indicate the polynomial degree. As the polynomial degree increases from $P = 2$ to $P = 4$, the fit to the reference case improves, as is expected. However, it seems there is more error in the mean value and quantiles when we move from $P = 4$ to $P = 5$ for both thrust and torque. This increase in the error has been explained further in Section 3.4 and Figure 6.

275 3.3 Choosing one surrogate model

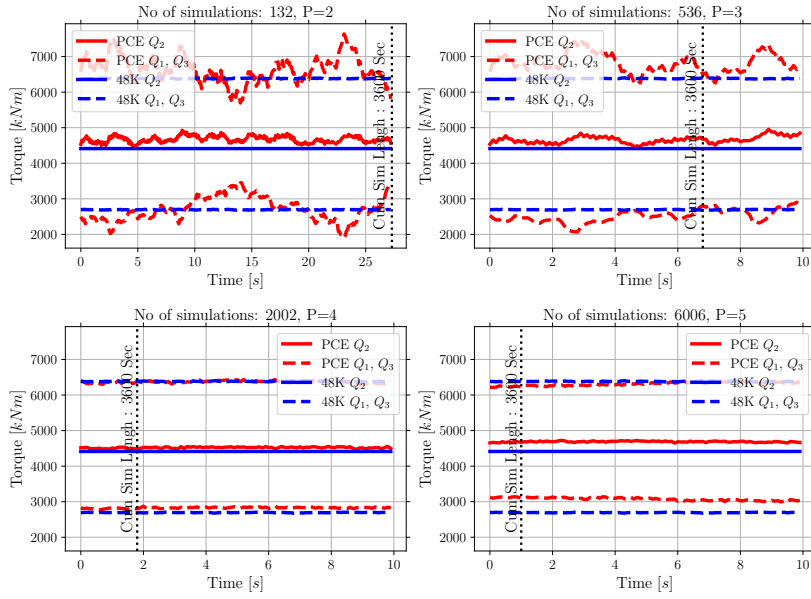
Building surrogate models aims to create an emulator that we can run quickly and provide statistics for the simulations without actually running the simulations. We initially ranked the surrogate models constructed for each time-step based on their mean values and standard deviations for each polynomial order separately to choose one surrogate model. As the surrogate models are PCEs, mean, standard deviation extraction is a simple step. After ranking the surrogate models, we selected the middle
280 surrogate model from the ranked succession for each polynomial order. That provided us 4 surrogate models for thrust and 4 surrogate models for torque, one per polynomial order.

3.4 Surrogate models accuracy

Next, we took the selected surrogate models thorough MCS of the surrogate models 10^6 times. Essentially, we took random samples from our 10 dimensional random domains 10^6 times and inserted those in the PCEs (Eq. (4) and Eq. (5)). The
285 MCS outputs are then used to check the surrogate model's accuracy. One can argue that this method is cherry-picking the surrogate models. This argument is valid for the low order ($P = 2, 3$) polynomial surrogate models. However, from Figure 4



(a) Thrust



(b) Torque

Figure 4. The Q_1 , Q_2 and Q_3 comparison from the reference case (48K simulations) and extracted values from PCEs for both trust and torque. The number of simulations used to build the PCEs and polynomial degree P are mentioned on the plots. The cumulative data length of 3600s sufficient to build surrogates is shown with the vertical line.

we know these polynomial are not accurate regardless of which one we choose. This inaccuracy is more visible in Figure 6. For polynomials of orders 4 and 5, referring to Figure 4, the polynomial selection procedure induces an insignificant effect on the statistics.

290 To verify the surrogate models' accuracy, we use the Hellinger distance explained in section 2. This time, the Hellinger distance would show the difference between the surrogate model's 10^6 MCS outputs per polynomial order with the reference case at every time step. This procedure provides a vector of Hellinger distances for each polynomial degree where the vector's length is the same as the number of time steps in the simulations. As Hellinger distance is sensitive to binning, the bins are identical for each polynomial order surrogate model outputs. The same bins were used to calculate the reference simulations' histograms at each time step. Figure 5 shows the average Hellinger distance changes within a narrow band for each polynomial degree. The Hellinger distance becomes smaller as the polynomial degree increases, which is expected.

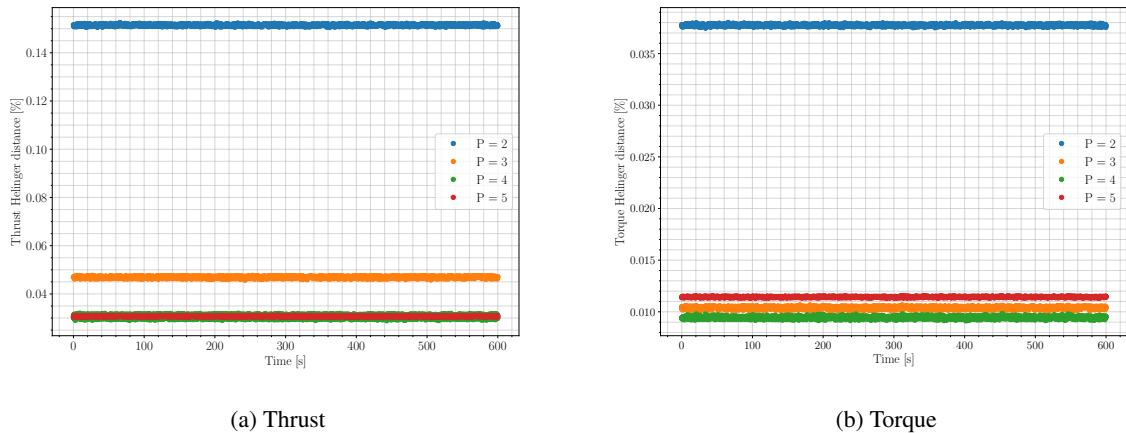


Figure 5. Hellinger distance between the different polynomial order surrogate models for one million MCS of the selected thrust and torque surrogates and the reference case simulations $48K$ at every time step

Afterwards, we compare the histogram of those with one arbitrary time step of the reference case of 48000 simulations. For each polynomial degree, regardless of the reference case time-step location in the time series, the difference between the reference case and the MCS only depends on the polynomial order. In other words, the difference between the MCS result histogram and the reference case histogram was only dependent on the polynomial degree and not the position of the time-step in the time series as expected for a stationary process. Figure 6 compares the histogram of 10^6 MCS for the middle mean ranked surrogate model to the reference case at one arbitrary time step for four polynomial degrees.

Figure 6 shows how the surrogate models match the simulations output histogram. It is visible that the polynomials order $P = 3$ and $P = 4$ can cover the non-linearity in the results, while the second-order polynomial cannot. Polynomial order $P = 5$ does not work well for both thrust and torque. Although we met the rule of thumb for the number of simulations as mentioned in Table 1, this shows an *under fit* for $P = 5$. This means more simulations are required to make the fit feasible. Both Figures 5 and 6 show that $P = 4$ provides an acceptable accuracy for the surrogate models. Therefore, further tests on the surrogate models

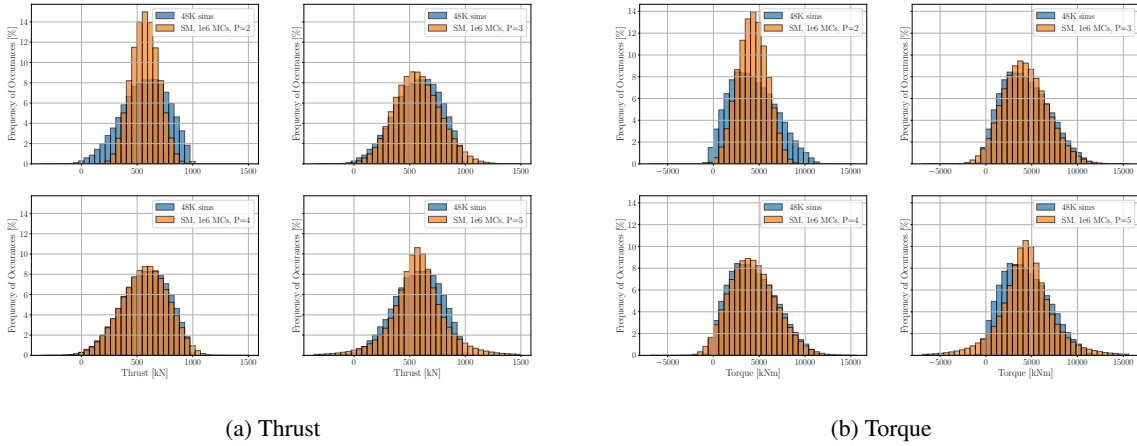


Figure 6. Thrust and torque Surrogate models with one million MCS vs the reference case histogram

with $P = 5$ appear unnecessary. From Figures 5 and 6 we can conclude that the PCE surrogate model with polynomial order $P = 4$ is accurate enough to emulate the aerodynamic model with an acceptable accuracy, while covering its non-linearity.

310 Another metric to show the accuracy of the surrogate model is Normalized Root Mean Square Error (NRMSE) also known as L_2 norm error. The NRMSE is calculated for every time step for the first $10s$ by running MCS for the surrogate model $P = 4$ for the same input as the reference case simulations. This means we use the same samples we took from the $10 - D$ random variables to generate the unsteady wind and then calculate the $48K$ reference case to run the surrogate model MCS. Figure 7 shows the error against time. As expected and visible from Figure 4 the NRMSE is higher for torque and lower for thrust.

315 In both cases, the maximum NRMSE is less than 10%. This error deemed acceptable as the surrogate model aims to provide overall accurate statistics and not point-to-point accuracy in the estimation and is necessarily a trade-off between speed and accuracy in the intended applications.

Figures 5, 6 and 7 show the PCE surrogate model has succeeded with the samples from the $10 - D$ uniform distribution and converts them to a Weibull distribution for both thrust and torque. Also, this proves the ability of the PCE surrogate in this

320 study to deal with the inherent non-linearity of the combination of unsteady wind generation and aerodynamic model together.

3.5 Surrogate model efficiency

Building the surrogate models aims to emulate the output of the actual model in an accurate and computationally efficient fashion. To inspect success in this respect, we start with registering the computation time required to run 2002, 6006 and reference case $48K$, $600s$ aerodynamic simulations. The previous section shows that we do not need the $600s$ length simulations

325 to build the surrogate models. Based on what we showed in Section 3.4, the required time to run $1s$ simulations (10 time steps) and building one surrogate model are provided. The computational time in Table 2 includes the unsteady wind generation. Additionally, we record the time required to build one surrogate model. The time to build one surrogate model for both thrust and torque is similar, and the average is provided here. As IEC standards (IEC 61400-1) asks for at least six aerodynamic

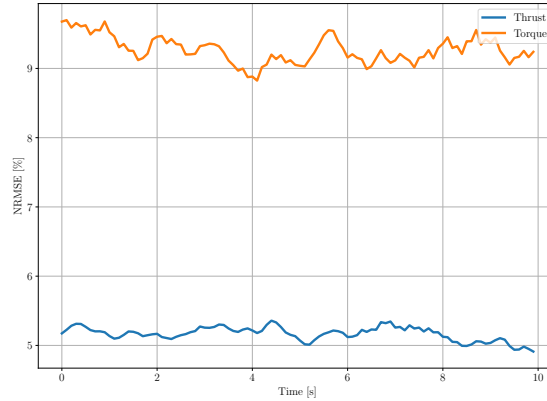


Figure 7. Surrogate models $P = 4$ NRMSE for both Thrust and Torque with respect to the reference case

simulations per average wind speed, we register the time for that set of aerodynamic simulations also. We perform aerodynamic simulations and surrogate model building on Compute Canada WestGrid clusters. The CPU time for the aerodynamic simulations and building the surrogate models is presented in Table 2.

Table 2. The computational time required to run aerodynamic simulations and building the surrogate models

Case	No of aerodynamic sims	Simulation length	Computation time	Time required build 1 surrogate models
Sims for PCE $P = 4$	2002	1s	10s	1min 2s
Sims for PCE $P = 5$	6006	1s	31s	15min 54s
Common practice	6	600s	18.62s	N/A
Reference case	48000	600s	41h 55min 48s	N/A

The computational time to build one surrogate model is long for $P = 5$. This is due to employing the point collocation method to calculate the PCEs coefficients. The point collocation method is inherently a regression method, using least squares to minimize the error (Feinberg and Langtangen, 2015).

After building the surrogate models, we ran large sets of MCS for the PCE surrogate models with the polynomial order 4 (as it is the most accurate one) and tracked the required time to run the MCS. All the MCS were performed on Compute Canada WestGrid clusters. The computation time for the MCS is shown in Table 3. As the computational time difference between thrust and torque is insignificant, the one which took longer is mentioned here.

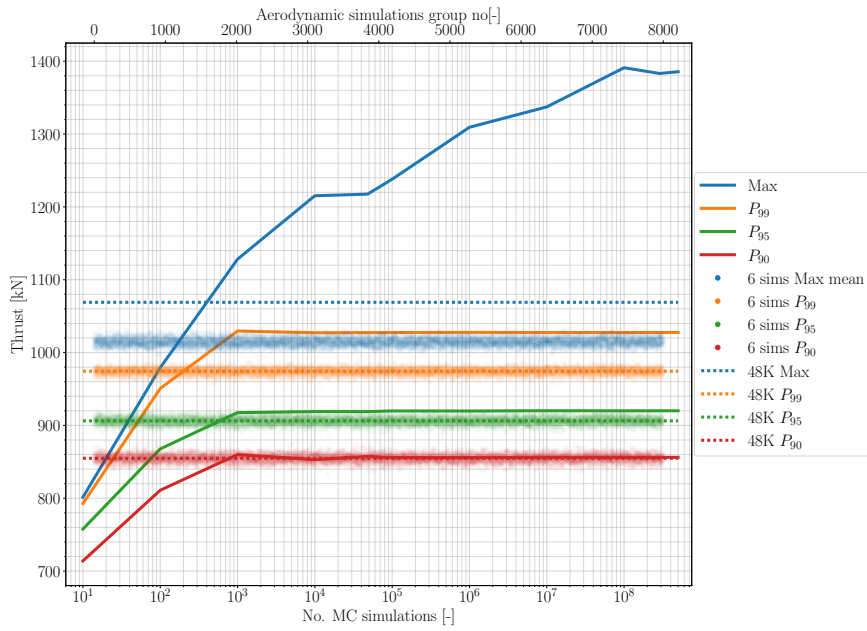
The number of time steps in the reference case is 288 M (6000 time-steps multiplied into 48000 aerodynamic simulations). Therefore, to have a fair comparison we can compare computational time for the reference case in Table 2 with 288 M MCS in Table 3. Adding up the computational time required for the surrogate model input simulations and building the surrogate model, still, the MCS is more efficient by a big margin.

Table 3. The computational time registered for to run MCS on the surrogate models with the polynomial order 4.

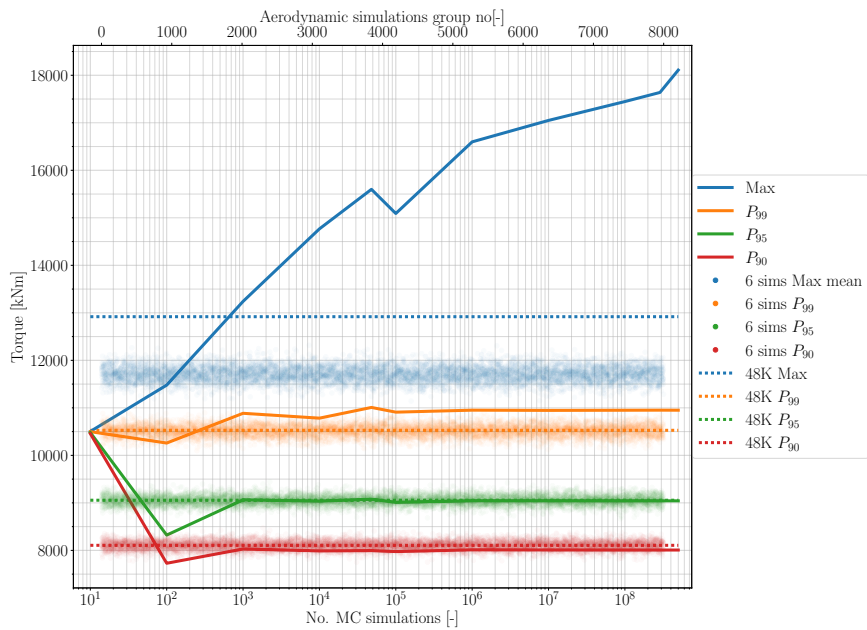
No. MCS simulations	Surrogate model $P = 4$
10, 100, 1K	< 0.1s
10 K	< 0.25s
48 K	0.85s
100 K	1.70s
1 M	30.84s
10 M	5min 51s
100 M	55min 33s
288 M	2h 40min 1s
500 M	4h 46min 36s

The ease of running MCS provides the ability to have more samples from the random domain. More samples from the random domain cover more of the statistical domain and capture the extreme loads more efficiently than running time marching aerodynamic simulations and extrapolation. Figure 8 presents the comparison between different MCS and the reference case aerodynamic simulations, maximum, 99th percentile P_{99} , 95th percentile P_{95} and 90th percentile P_{90} . The maximum load and the percentiles extracted from the $P = 4$ surrogate models run for both thrust and torque shown in relation to the number of MCS.

According to IEC standards (IEC 61400-1), the maximum load needs to be calculated based on the mean of the max (mean-max) of at least six seeds of unsteady wind aerodynamic simulations per average wind speed. Therefore, we randomly grouped the reference case simulations (48K simulations) into 8000 unique groups to have a fair comparison with the common practice. Afterwards, the mean of the max per group, and the 90th percentile P_{99} , 95th percentile P_{95} and 90th percentile P_{90} of each group is calculated. These data are presented in Figure 8 as clouds of dots for both thrust and torque.



(a) Thrust



(b) Torque

Figure 8. Maximum load and percentile comparison between the aerodynamic simulations reference case, the MCS and groups aerodynamic simulations for thrust and torque

To extract the maximum value that matches the reference case aerodynamic simulations, we need to run a large number of
355 MCS. Figure 8a and 8b show for the PCE order 4 the maximum thrust and torque from the MCS matches the reference case
around almost 1000 MCS. Looking at P_{99} , P_{95} and P_{90} for both surrogate models, the convergence happen at around the same
number of MCS. Figures 8a and 8b show after 1K or 100K MCS the percentiles are close to the reference case. Interestingly,
the mean-max output from the grouped aerodynamic simulations has a wide distribution. This shows the inaccuracy of looking
at a small number of simulations to calculate the extreme loads. This distribution is smaller for the percentile data; however,
360 it is not comparable with the convergence of MCS outputs. Also, looking at the grouped simulations output, and compared to
the standard practice (mean-max) and P_{99} , illustrates the conservative design approach of the IEC standards (IEC 61400-1).

Referring to the computational time required to build the surrogate model and then running the MCS, these plots show
promising results to extract accurate extreme loads from the surrogate models in a computationally efficient manner.

4 Conclusion

365 This paper's aim is to build a non-intrusive surrogate model of time marching aerodynamic simulations. The form of the
surrogate model used in this paper is a PCE. In Section 2, we explained the aerodynamic model used for this study. Then,
we briefly described the method that we are using to build the PCEs. One major challenge with the building of the surrogate
models is the *curse of dimensionality*, which we tried to tackle by using a reduced Veers model.

We showed how by increasing the number of simulations, the results' statistics converge and do not change in time. As a
370 result, building a few accurate surrogate models, or even one, for a small length of time would suffice for our purpose. In other
words, the time does not have any meaning in the sectional statistics. Therefore, to build an accurate surrogate model, we can
significantly reduce the simulation length while increasing the number of the simulation. In the results section, we showed the
surrogate model using a fourth-order polynomial built on 2002 simulations with a length of 2s gives us sufficiently accurate
results in large MC runs to obtain output statistics. Afterwards, we demonstrate the surrogate model's efficiency by comparing
375 the computational time required to run the aerodynamic simulations and build the surrogate model with the required time for
running MCS to have accurate statistics. Also, we show the high percentile values extracted from the MCS match the reference
case with a relatively low number of MCS and thus computationally efficient.

The BEM-based aerodynamic model approach is well known in the literature and research. We choose 30s transient time for
the simulations to ensure they do not include any transition results. As the model is a simplified BEM it is quick to run, and this
380 is not a challenge. However, for future work with actual aeroelastic codes (e.g. FAST), a smart way to deal with initialization
time is essential; otherwise, increasing the number of simulations and the model complexity would be very expensive. For
example, if the required initialization time is 60s (default in FAST), and we want to increase the number of simulations from
6 six hundred second simulations (minimum requirement according to IEC 61400-1) to 6006 two-second simulations, we are
not doing any good in terms of computational cost. Aeroelastic and longer wakes will be studied for this challenge and blended
385 or common initialization period trialled.

Another challenge is the practical application of this surrogate model. The surrogate model that we build in this study is one or a few time steps, each inherently the same due to the statistical similarity. If we want to build one time series from this surrogate model, we have to sample the 10 dimensional random domain for the number of time steps to have a time series to post-process. For example, suppose we want to have a 600s time series of thrust or torque with the time step of 0.1s for the aerodynamic model that we developed in this study. In that case, we need to take 6000 samples from the 10 dimensional uniform distribution random domain, and run MCS for each. However, this would provide us with 6000 thrust and torque values, which will miss the auto-correlation, which is inherent in the generated unsteady wind, in the results. This drawback is crucial if we, for instance, want to calculate fatigue loads from the surrogate model. This challenge will require a surrogate form capable of resolving the correlation between time-steps. Fluck and Crawford (2018) did this previously for intrusive PCEs of an aerodynamic model, however as mentioned before, that can get very complicated for more advanced models.

Using non-conventional polynomials, such as what Fluck and Crawford (2018) did, might result in a more efficient polynomial that requires fewer number simulations to build the surrogate model. Finally, we want to implement the method on commercial wind turbine simulation packages such as FAST to test the approach in future work. It is important to again note however that the physics model used in the current work is equivalent to FAST, just conveniently formulated in Python for our surrogate model development efforts.

The notion of the "reduced Veers model" would work for the aerodynamic simulations we used in this study. However, this reduced model would not be efficient and sufficient to move towards commercial wind turbine packages. Therefore, a new approach to reduce the data in a "turbulence box" Jonkman (2009) spatially and temporally would be necessary. Similar work has been done in Guo and Ganapathysubramanian (2017) and will be explored.

Code and data availability. The code and data that support the findings of this study are available from the corresponding author, RH, upon request.

Author contributions. RH developed the necessary computer code and wrote the paper in consultation with and under the supervision of CC.

Competing interests. The authors confirm there are no competing interests present.

Acknowledgements. We greatly acknowledge the funding for this study by the Natural Sciences and Engineering Research Council of Canada (NSERC). This research was enabled in part by support provided by WestGrid (www.westgrid.ca) and Compute Canada Canada (www.computecanada.ca).

References

- Ashuri, T., Zhang, T., Qian, D., and Rotea, M.: Uncertainty quantification of the levelized cost of energy for a 20 MW research wind turbine model, in: 34th Wind Energy Symposium, p. 1998, 2016.
- 415 Barlas, T., Ramos-García, N., Pirrung, G. R., and González Horcas, S.: Surrogate-based aeroelastic design optimization of tip extensions on a modern 10 MW wind turbine, *Wind Energy Science*, 6, 491–504, 2021.
- Basu, A., Shioya, H., and Park, C.: *Statistical Inference: The Minimum Distance Approach*, Chapman & Hall/CRC Monographs on Statistics & Applied Probability, CRC Press, 2011.
- Bossanyi, E.: GH bladed theory manual, GH & Partners Ltd, 2, 56–58, 2003.
- 420 Bossanyi, E., Burton, T., Sharpe, D., and Jenkins, N.: *Wind energy handbook*, New York: Wiley, 2011.
- Dimitrov, N.: Surrogate models for parameterized representation of wake-induced loads in wind farms, *Wind Energy*, 22, 1371–1389, 2019.
- Dimitrov, N., Kelly, M., Vignaroli, A., and Berg, J.: From wind to loads: wind turbine site-specific load estimation using databases with high-fidelity load simulations, *Wind Energy Science Discussions*, 2018, 1–39, <https://doi.org/10.5194/wes-2018-18>, 2018.
- Eldred, M., Webster, C., and Constantine, P.: Evaluation of non-intrusive approaches for Wiener-Askey generalized polynomial chaos, in: 425 10th AIAA Non-Deterministic Approaches Conference, p. 1892, 2008.
- Feinberg, J. and Langtangen, H. P.: Chaospy: An open source tool for designing methods of uncertainty quantification, *Journal of Computational Science*, 11, 46–57, 2015.
- Fluck, M. and Crawford, C.: Fast analysis of unsteady wing aerodynamics via stochastic models, *AIAA Journal*, 55, 719–728, 2016a.
- Fluck, M. and Crawford, C.: A stochastic aerodynamic model for stationary blades in unsteady 3D wind fields, in: *Journal of Physics: Conference Series*, vol. 753, p. 082009, IOP Publishing, 2016b.
- 430 Fluck, M. and Crawford, C.: An engineering model for 3-D turbulent wind inflow based on a limited set of random variables, *Wind Energy Science*, 2, 507–520, <https://doi.org/10.5194/wes-2-507-2017>, 2017.
- Fluck, M. and Crawford, C.: A fast stochastic solution method for the Blade Element Momentum equations for long-term load assessment, *Wind Energy*, 21, 115–128, 2018.
- 435 Ghanem, R., Higdon, D., and Owhadi, H.: *Handbook of uncertainty quantification*, Springer, 2017.
- Ghanem, R. G. and Spanos, P. D.: *Stochastic finite elements: a spectral approach*, Courier Corporation, 2003.
- Guo, Q. and Ganapathysubramanian, B.: Incorporating a stochastic data-driven inflow model for uncertainty quantification of wind turbine performance, *Wind Energy*, 20, 1551–1567, 2017.
- Hellinger, E.: Neue begründung der theorie quadratischer formen von unendlichvielen veränderlichen., *Journal für die reine und angewandte* 440 *Mathematik (Crelles Journal)*, 1909, 210–271, 1909.
- Hosder, S., Walters, R., and Balch, M.: Efficient sampling for non-intrusive polynomial chaos applications with multiple uncertain input variables, in: 48th AIAA/ASME/ASCE/AHS/ASC Structures, Structural Dynamics, and Materials Conference, p. 1939.
- IEC 61400-1: Wind energy generation systems - Part 1: Design requirements, Standard, International Electrotechnical Commission, 2019.
- Jonkman, B. J.: *TurbSim user's guide: Version 1.50*, 2009.
- 445 Jonkman, J., Butterfield, S., Musial, W., and Scott, G.: Definition of a 5-MW reference wind turbine for offshore system development, Tech. rep., National Renewable Energy Lab.(NREL), Golden, CO (United States), 2009.
- Jonkman, J. M., Buhl Jr, M. L., et al.: *FAST user's guide*, 2005.

- Kaintura, A., Dhaene, T., and Spina, D.: Review of Polynomial Chaos-Based Methods for Uncertainty Quantification in Modern Integrated Circuits, Electronics, 7, 30, 2018.
- 450 Kim, S. H. and Boukouvala, F.: Machine learning-based surrogate modeling for data-driven optimization: a comparison of subset selection for regression techniques, Optimization Letters, pp. 1–22, 2019.
- Kucherenko, S., Albrecht, D., and Saltelli, A.: Exploring multi-dimensional spaces: a Comparison of Latin Hypercube and Quasi Monte Carlo Sampling Techniques, 2015.
- Larsen, T. J. and Hansen, A. M.: How 2 HAWC2, the user’s manual, 2007.
- 455 Le Maître, O. and Knio, O. M.: Spectral methods for uncertainty quantification: with applications to computational fluid dynamics, Springer Science & Business Media, 2010.
- Lupton, R.: Frequency-domain modelling of floating wind turbines, Ph.D. thesis, University of Cambridge, 2015.
- Lupton, R.: bemused, <https://github.com/ricklupton/bemused>, 2019.
- Murcia, J. P., Réthoré, P.-E., Dimitrov, N., Natarajan, A., Sørensen, J. D., Graf, P., and Kim, T.: Uncertainty propagation through an aeroelastic
- 460 wind turbine model using polynomial surrogates, Renewable Energy, 119, 910–922, 2018.
- Niederreiter, H.: Random Number Generation and Quasi-Monte Carlo Methods, Society for Industrial and Applied Mathematics, <https://doi.org/10.1137/1.9781611970081>, 1992.
- Rao, S. S.: A course in time series analysis, 2008.
- Schröder, L., Dimitrov, N. K., Verelst, D. R., and Sørensen, J. A.: Wind turbine site-specific load estimation using artificial neural networks
- 465 calibrated by means of high-fidelity load simulations, in: Journal of Physics: Conference Series, vol. 1037, p. 062027, IOP Publishing, 2018.
- Schröder, L., Dimitrov, N. K., and Sørensen, J. A.: Uncertainty propagation and sensitivity analysis of an artificial neural network used as wind turbine load surrogate model, in: Journal of Physics: Conference Series, vol. 1618, p. 042040, IOP Publishing, 2020a.
- Schröder, L., Dimitrov, N. K., and Verelst, D. R.: A surrogate model approach for associating wind farm load variations with turbine failures,
- 470 Wind Energy Science, 5, 1007–1022, 2020b.
- Slot, R. M., Sørensen, J. D., Sudret, B., Svenningsen, L., and Thøgersen, M. L.: Surrogate model uncertainty in wind turbine reliability assessment, Renewable Energy, 151, 1150–1162, 2020.
- Smolyak, S.: Quadrature and interpolation formulas for tensor products of certain classes of functions, in: Soviet Math. Dokl., vol. 4, pp. 240–243, 1963.
- 475 Sobol’, I. M.: On the distribution of points in a cube and the approximate evaluation of integrals, Zhurnal Vychislitel’noi Matematiki i Matematicheskoi Fiziki, 7, 784–802, 1967.
- Sudret, B.: Uncertainty propagation and sensitivity analysis in mechanical models—Contributions to structural reliability and stochastic spectral methods, Ph.D. thesis, 2007.
- Sudret, B.: Polynomial chaos expansions and stochastic finite element methods, Risk and reliability in geotechnical engineering, pp. 265–300,
- 480 2015.
- Tyson, S., Donovan, D., Thompson, B., Lynch, S., and Tas, M.: Uncertainty Modelling with Polynomial Chaos Expansion: Stage 1 - Final Report, 2015.
- van den Bos, L., Sanderse, B., Blonk, L., Bierbooms, W., and van Bussel, G.: Efficient ultimate load estimation for offshore wind turbines using interpolating surrogate models, in: Journal of Physics: Conference Series, vol. 1037, p. 062017, IOP Publishing, 2018.

- 485 van Garrel, A.: Development of a Wind Turbine Aerodynamics Simulation Module, Tech. rep., Energy research Centre of the Netherlands, <https://doi.org/10.13140/RG.2.1.2773.8000>, 2003.
- Veers, P. S.: Three-dimensional wind simulation, Tech. rep., Sandia National Labs., Albuquerque, NM (USA), 1988.
- Wang, H., Jiang, X., Chao, Y., Li, Q., Li, M., Chen, T., and Ouyang, W.: Numerical optimization of horizontal-axis wind turbine blades with surrogate model, *Proceedings of the Institution of Mechanical Engineers, Part A: Journal of Power and Energy*, p. 0957650920976743, 490 2020.
- Xiu, D. and Karniadakis, G. E.: The Wiener–Askey polynomial chaos for stochastic differential equations, *SIAM journal on scientific computing*, 24, 619–644, 2002.
- Xiu, D. and Karniadakis, G. E.: Modeling uncertainty in flow simulations via generalized polynomial chaos, *Journal of computational physics*, 187, 137–167, 2003.
- 495 Xiu, D., Lucor, D., Su, C.-H., and Karniadakis, G. E.: Stochastic modeling of flow-structure interactions using generalized polynomial chaos, *Journal of Fluids Engineering*, 124, 51–59, 2002.